JOURNAL OF BACTERIOLOGY, Mar. 2007, p. 1765–1773 Vol. 189, No. 5
0021-9193/07/$08.00+0 doi:10.1128/JB.00776-06

The *pio* Operon Is Essential for Phototrophic Fe(II) Oxidation in *Rhodopseudomonas palustris* TIE-1[▽]

Yongqin Jiao[1] and Dianne K. Newman[1,2,3]*

Division of Geological and Planetary Sciences,[1] Division of Biology,[2] and Howard Hughes Medical Institute,[3] California Institute of Technology, Pasadena, California

Received 30 May 2006/Accepted 12 December 2006

Phototrophic Fe(II)-oxidizing bacteria couple the oxidation of ferrous iron [Fe(II)] to reductive CO_2 fixation by using light energy, but until recently, little has been understood about the molecular basis for this process. Here we report the discovery, with *Rhodopseudomonas palustris* TIE-1 as a model organism, of a three-gene operon, designated the *pio* operon (for *p*hototrophic *i*ron *o*xidation), that is necessary for phototrophic Fe(II) oxidation. The first gene in the operon, *pioA*, encodes a *c*-type cytochrome that is upregulated under Fe(II)-grown conditions. PioA contains a signal sequence and shares homology with MtrA, a decaheme *c*-type cytochrome from *Shewanella oneidensis* MR-1. The second gene, *pioB*, encodes a putative outer membrane beta-barrel protein. PioB is a homologue of MtrB from *S. oneidensis* MR-1. The third gene, *pioC*, encodes a putative high potential iron sulfur protein (HiPIP) with a twin-arginine translocation (Tat) signal sequence and is similar to the putative Fe(II) oxidoreductase (Iro) from *Acidithiobacillus ferrooxidans*. Like PioA, PioB and PioC appear to be secreted proteins. Deletion of the *pio* operon results in loss of Fe(II) oxidation activity and growth on Fe(II). Complementation studies confirm that the phenotype of this mutant is due to loss of the *pio* genes. Deletion of *pioA* alone results in loss of almost all Fe(II) oxidation activity; however, deletion of either *pioB* or *pioC* alone results in only partial loss of Fe(II) oxidation activity. Together, these results suggest that proteins encoded by the *pio* operon are essential and specific for phototrophic Fe(II) oxidation in *R. palustris* TIE-1.

One of the distinguishing features of microbial metabolism is its diversity: over billions of years of Earth history, microbes have evolved an impressive array of strategies to obtain energy for growth. The process of photosynthesis, for example, goes well beyond the ability to split water and produce oxygen. Different groups of microorganisms carry out "anoxygenic" photosynthesis by using substrates such as molecular hydrogen (H_2), various sulfur species, small organic molecules, or ferrous iron [Fe(II)] as an exogenous electron donor to drive reductive CO_2 fixation (6, 8, 12, 17). If we seek to understand the origins of the remarkable metabolic diversity that characterizes modern life on Earth, it is important to know how different types of metabolisms operate at the molecular level. This is necessary both to be able to compare the components of different metabolisms to each other and to inform our search for biosignatures unique to these metabolisms in the rock record.

As a step toward this general goal, we have chosen to focus on the process of phototrophic Fe(II) oxidation, which can be described by the following equation: $4Fe^{2+} + CO_2 + 11H_2O + h\nu = [CH_2O] + 4Fe(OH)_3 + 8H^+$. This type of photosynthesis is interesting in the context of metabolic evolution for several reasons. First, phototrophic Fe(II) oxidation is phylogenetically widespread, appearing in purple and green bacteria (10, 14, 21, 22, 65, 66); phylogenic comparisons of genes from different photosynthetic organisms suggest that anoxygenic photosynthesis is more ancient than oxygenic photosynthesis (57, 72). Second, iron has an intermediate redox potential ($\Delta E_0' = -0.11$ V) (28) compared to other substrates used as electron donors in photosynthesis [e.g., H_2 ($\Delta E_0' = -0.41$ V) or H_2O ($\Delta E_0' = 0.82$ V)] (28, 44). It has been suggested, therefore, that Fe(II)-based photosynthesis may represent a transition form of metabolism from anoxygenic to oxygenic photosynthesis (57). Third, Fe(II) is thought to have been the most widespread source of reducing power in the late Archean and early Proterozoic (3.8 to 1.6 billion years ago) with an estimated concentration of about 0.1 to 1 mM in seawater (69); atmospheric oxygen seems to have appeared in significant amounts only after 2.4 billion years ago (Ga) (15, 26, 30, 60).

Banded iron formations (BIFs) are an ancient class of iron ore deposits that may record the story of the evolution of photosynthesis. Because the use of Fe(II) results in the production of ferric iron [Fe(III)] minerals, it has been suggested that Fe(II)-based phototrophy might have been responsible for catalyzing BIF deposition early in Earth history (14, 34, 71). Later occurrences of BIFs (e.g., at 1.8 Ga), however, are believed to have resulted from Fe(II) oxidation catalyzed by molecular oxygen produced by cyanobacteria. Episodic deposition of BIFs throughout the Precambrian thus may reflect a transition from anoxygenic to oxygenic photosynthesis. How did ancient phototrophs evolve from using Fe(II) as an electron donor to using H_2O?

To address this question, we must understand the molecular machinery of phototrophic Fe(II) oxidation. Discovered in the early 1990s by Widdel and coworkers (71), phototrophic Fe(II)-oxidizing bacteria such as *Thiodictyon*, *Rhodobacter*, and *Chlorobium* species have been isolated from a wide variety of environments, including both freshwater and marine settings

* Corresponding author. Mailing address: California Institute of Technology, Division of Geological and Planetary Sciences, Mail Stop 100-23, Pasadena, CA 91125. Phone: (626) 395-6790. Fax: (626) 683-0621. E-mail: dkn@gps.caltech.edu.

▽ Published ahead of print on 22 December 2006.

TABLE 1. Bacterial strains and plasmids used in this study

Strain or plasmid	Genotype, markers, or characteristics[a]	Source or reference
E. coli strains		
WM3064	Donor strain for conjugation; *thrB1004 pro thi rpsL hsdS lacZ*ΔM15 RP4-1360 Δ(*araBAD*)*567* Δ*dapA1341*::[*erm pir* (wt)]	W. Metcalf, University of Illinois, Urbana
UQ950	*E. coli* DH5α (*pir*) host for cloning; F^- Δ(*argF-lac*)*169* Φ*80dlacZ58*(ΔM15) *glnV44*(As) *rfbD1 gyrA96*(Nal^r) *recA1 endA1 spoT1 thi-1 hsdR17 deoR* λ*pir*$^+$	D. Lies, Caltech
S17-1	*thi pro hdsR hdsM*$^+$ *recA*; chromosomal insertion of RP4-2 (Tc::Mu Km::Tn*7*)	63
R. palustris strains		
TIE-1	Isolated from Woods Hole, MA	28
CGA009	Wild type (ATCC BAA-98)	32
CGA010	*hupV*$^+$ derivative of CGA009	F. Rey and C. S. Harwood, University of Washington
TIE-3	*R. palustris* TIE-1 Δ*pioABC*	This study
Δ*pioA*	*R. palustris* TIE-1 Δ*pioA*	This study
Δ*pioB*	*R. palustris* TIE-1 Δ*pioB*	This study
Δ*pioC*	*R. palustris* TIE-1 Δ*pioC*	This study
Plasmids		
pJQ200SK	Mobilizable suicide vector; *sacB* Gm^r	59
pYQABC	2-kb fusion PCR fragment containing Δ*pioABC* cloned into SpeI site of pJQ200sk; used to make TIE-3 Δ*pioABC* strain	This study
pYQA	2-kb fusion PCR fragment containing Δ*pioA* cloned into SpeI site of pJQ200sk; used to make TIE-4 Δ*pioA* strain	This study
pYQB	2-kb fusion PCR fragment containing Δ*pioB* cloned into SpeI site of pJQ200sk; used to make TIE-5 Δ*pioB* strain	This study
pYQC	2-kb fusion PCR fragment containing Δ*pioC* cloned into SpeI site of pJQ200sk; used to make TIE-6 Δ*pioA* strain	This study
pBBR1MCS-2	5.1-kb broad-host range plasmid; Km^r *lacZ*	31
pYQ01	PCR fragment, including *pioABC*, generated with primers cyc-start and FeS-end, cloned into HindIII and SpeI sites of pBBR1MCS-2	This study
pYQ02	PCR fragment, including *pioA*, generated with primers cyc-start and cyc-end, cloned into HindIII and SpeI sites of pBBR1MCS-2	This study
pYQ03	PCR fragment, including *pioB*, generated with primers MtrB-start and MtrB-end, cloned into HindIII and SpeI sites of pBBR1MCS-2	This study
pYQ04	PCR fragment, including *pioC*, generated with primers FeS-start and FeS-end, cloned into HindIII and SpeI sites of pBBR1MCS-2	This study

[a] Km, kanamycin; Gm, gentamicin.

(14, 21, 29, 66, 71). However, very little is understood at the molecular level about the mechanism of Fe(II) oxidation in any of these organisms. In the companion paper to this article, we report the discovery of a *c*-type cytochrome and a putative pyrroloquinoline quinone-containing enzyme from an Fe(II)-oxidizing strain—*Rhodobacter* sp. strain SW2—that stimulate Fe(II) oxidation activity in its close relative *Rhodobacter capsulatus* SB1003 (11). Because our ability to explore the mechanistic basis of Fe(II) oxidation in SW2 is limited because of the impracticality of direct mutational analysis (11), we established a genetic system in a different Fe(II)-oxidizing phototroph, *Rhodopseudomonas palustris* TIE-1 (28). In this report, we describe the identification of the *pio* operon, a three-gene operon essential for phototrophic growth on Fe(II) by *R. palustris* TIE-1.

MATERIALS AND METHODS

Bacterial strains and plasmids. The bacterial strains and plasmids used in this study are listed in Table 1. *R. palustris* CGA010, derived from parent strain CGA009 after a frameshift in the *hupV* gene was repaired, was kindly provided by F. Rey and C. S. Harwood (University of Washington).

Media and culture conditions. For aerobic growth *R. palustris* strains were grown in YP medium (0.3% yeast extract and 0.3% Bacto Peptone [Difco]) with shaking at 30°C. For anaerobic growth, *R. palustris* strains were grown without shaking at 30°C in FEM, a defined basal medium for phototrophic, Fe(II)-oxidizing bacteria (12). For photoheterotrophic growth, FEM was supplemented with 10 mM acetate. For photoautotrophic growth, electron donors such as thiosulfate (10 mM), hydrogen (80% atmosphere), and soluble Fe(II) were used. FEM medium containing soluble Fe(II) was prepared as previously described, and the final Fe(II) concentration is in the range of 4 to 6 mM (28). Cultures were incubated 20 to 30 cm from a 34-W tungsten incandescent light source at 30°C. All phototrophic cultures, except those grown on hydrogen, were grown in an atmosphere consisting of 80% N_2 and 20% CO_2. *Escherichia coli* strains were cultured in lysogeny broth (LB) at 37°C. *E. coli* WM3064 was supplemented with 300 μM diaminopimelic acid. Kanamycin and gentamicin were used at 100 and 200 μg/ml for *R. palustris* and 50 and 20 μg/ml for *E. coli*, respectively.

Cell suspension assay. All cell suspension assays were conducted at room temperature in an anaerobic chamber containing an atmosphere of 80% N_2, 15% CO_2, and 5% H_2 (12, 28). Fe(II) cultures used for this assay contained 10 mM nitrilotriacetic acid (NTA) to prevent ferric iron precipitation. NTA alone does not support phototrophic growth of *R. palustris* (data not shown). Cells were pregrown in the medium indicated until mid-exponential phase to an optical density (OD) at 660 nm of ~0.3 measured by 96-well plate reader (Synergy HT; Bio-Tek, Winooski, VT) with a volume of 200 μl. Cells were harvested by centrifugation (10,000 × *g* for 15 min) and washed in the same volume of HEPES buffer (50 mM HEPES, 20 mM NaCl, pH 7.0). To start the assay, cells were resuspended in HEPES buffer containing 20 mM $NaHCO_3$ and either 400 μM or 1 mM (as indicated in Fig. 1) $FeCl_2$. Cells were concentrated approximately three times compared to the original growth culture, and 100 μl of the cell suspension was aliquoted into a 96-well plate. The OD measured by the 96-well plate reader was about 0.7. The plates were incubated at room temperature in a glove box under a 40-W tungsten light with a light intensity of about 3,000 lx. Over time, 100 μl of ferrozine solution (1 g of ferrozine plus 500 g of ammonia acetate in 1 liter of double-distilled H_2O) was added to the wells to monitor Fe(II) levels (64). The rate of Fe(II) oxidation was calculated on the basis of the linear portion of the curves generated.

Extract preparation, sodium dodecyl sulfate-polyacrylamide gel electrophoresis (SDS-PAGE) analysis, and heme staining. *R. palustris* TIE-1 was grown on either H_2, thiosulfate, or Fe(II) plus NTA until mid-exponential phase, and cells were harvested by centrifugation at 10,000 × *g* for 15 min. Cell pellets were resuspended and washed three times in the same volume of HEPES buffer, resuspended in the same buffer containing protease inhibitor cocktail (Roche) and 50 μM DNase (Roche), and incubated at 4°C for 30 min. Cells were disrupted with a French press (three passes at 18,000 lb/in^2), and the cell lysate was clarified by centrifugation at 10,000 × *g* for 15 min at 4°C. The resulting supernatant was centrifuged at 200,000 × *g* for 120 min at 4°C. The supernatant

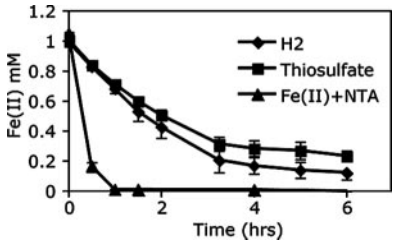

FIG. 1. Fe(II) oxidation activity of *R. palustris* TIE-1 tested by a cell suspension assay with cells pregrown phototrophically with Fe(II), H_2, or thiosulfate as the electron donor. Approximately 5×10^9 cells/ml were used in the cell suspension assay. Compared to the H_2- or thiosulfate-grown cells, Fe(II)-grown cells showed a four- to fivefold higher rate of Fe(II) oxidation activity, suggesting that specific proteins were induced under Fe(II)-grown conditions.

was defined as the soluble fraction, and the pellet, which was resuspended in HEPES buffer, was defined as the membrane fraction. Protein concentrations were determined by the Bradford assay (7). SDS-PAGE was preformed by standard procedures according to Laemmli (38). Soluble and membrane fractions were incubated in loading buffer containing dithiothreitol at room temperature for 10 min without heating and separated on a 12% Tris/HCl precast gel (Bio-Rad). Coomassie staining was performed by the Bio-Rad standard staining protocol as described by the manufacturer. Gels stained for heme-containing proteins were performed according to the in-gel peroxidase activity assay as previously described (16).

Reverse transcriptase (RT)-PCR. *R. palustris* TIE-1 was grown photoautotrophically on Fe(II) plus NTA until exponential phase. Total RNA was extracted as described previously (56). Briefly, cells were harvested and resuspended in 1 ml TE buffer (10 mM Tris/HCl, 1 mM EDTA, pH 8.0). Cells were disrupted with a Mini-BeadBeater-8 (BioSpec Products, Bartlesville, OK) in 2-ml screw-cap tubes containing approximately 1 ml of 0.1-mm zirconia-silica beads (BioSpec) for 1-min periods with cooling on ice after each period for a total of 4 min. RNA extraction was then carried out with a QIAGEN RNA extraction kit. DNase digestion was performed on the Mini-column with the QIAGEN RNase-free DNase set. The RNA was eluted from the column, and a second DNase treatment was performed with Roche RNase-free DNase. The RNA was finally resuspended in 40 μl nuclease-free water. cDNA was synthesized with a Bio-Rad iScript cDNA synthesis kit. A control PCR with RNA as the template in the absence of reverse transcriptase confirmed that the isolated RNA was free of contaminating genomic DNA. The primers used for all RT-PCRs are listed in Table 2. To test if *pioABC* were cotranscribed, primers RT-pioA-L1 and RT-pioB-R1 were used to detect the presence of transcript *pioAB* and primers RT-pioB-L1 and RT-pioC-R1 were used to detect transcript *pioBC*. To test the transcription of *pio* genes in the Δ*pioA*, Δ*pioB*, or Δ*pioC* mutant background, we used RT-pioAL and RT-pioAR to detect *pioA*, RT-pioBL and RT-pioBR to detect *pioB*, and RT-pioCL and RT-pioCR to detect *pioC*.

Cloning, DNA manipulations and mutant construction. Standard protocols were used for DNA cloning and transformation (28). Plasmids were purified on QIAprep spin columns (QIAGEN Inc., Chatsworth, CA). *R. palustris* TIE-1 chromosomal DNA was isolated with a DNeasy kit (QIAGEN). DNA was extracted from agarose gels with the QIAquick gel extraction kit (QIAGEN), and plasmid DNA was purified with the Qiaprep spin miniprep kit (QIAGEN). DNA was sequenced at the Laragen DNA sequencing center (http://www.laragen.com/services.htm) by standard automated-sequencing technology.

Construction of deletion mutant. All primer sequences used in construction of the mutants are listed in Table 2. For construction of *pio* operon deletion mutant TIE-3, a 1-kb DNA fragment upstream of *pioA* was produced by PCR with primers pioA1 and pioA1p with TIE-1 genomic DNA as the template. Similarly, a 1-kb PCR fragment downstream of *pioC* was generated with primers pioC2 and pioC2p. The PCR products were used as templates for another round of fusion PCR with primers pioA1 and pioC2. The resulting 2-kb fusion PCR product was gel purified and restriction digested with restriction enzyme SpeI and cloned into the suicide vector pJQ200sk (59) to generate pYQABC. pYQABC was mobilized into TIE-1 by conjugation from *E. coli* S17-1 (13). Selection of single recombinants on PM plates containing 400 μg/ml gentamicin, followed by selection of double recombinants on PM sucrose (10%) plates, were conducted as previously described (13). Individual Δ*pioA*, Δ*pioB*, and Δ*pioC* gene deletion mutants were made in a similar manner via suicide plasmids pYQA, pYQB, and pYQC, respectively. The primers used for generating pYQA were pioA1, pioA1p, pioA2, and pioA2p; those used for pYQB were pioB1, pioB1p, pioB2, and pioB2p; and those used for pYQC were pioC1, pioC1p, pioC2, and pioC2p. PCR was used to verify that the expected deletion had occurred.

Generation of complementing plasmids. The *pioABC* operon and the individual *pio* genes were amplified from genomic DNA of TIE-1 with the FailSafe PCR kit (Epicenter, WI). The PCR products were designed to have EcoRI and HindIII restriction sites and were ligated in *trans* into vector pBBRMCS-2 (35, 36) digested with the same enzymes. The resulting plasmids were conjugated into the *R. palustris* strains indicated as previously described (28). The *pioABC* operon was amplified with primers pioA-start and pioC-end (pYQ01), the *pioA* gene was amplified with primers pioA-start and pioA-end (pYQ02), the *pioB* gene was amplified with primers pioB-start and pioB-end (pYQ03), and the *pioC* gene was amplified with primers pioC-start and pioC-end (pYQ04).

Nucleotide sequence accession numbers. The DNA sequences of *pioA*, *pioB*, and *pioC* were deposited in the GenBank database under accession numbers EF119739, EF119740, and EF119741, respectively.

RESULTS

Identification of an Fe(II) oxidation-specific *c*-type cytochrome. With the goal of identifying proteins that are expressed when TIE-1 grows on Fe(II), we compared the Fe(II) oxidation activity of cell suspensions that had been pregrown photoautotrophically on different electron donors including H_2, thiosulfate, and Fe(II). Cells were collected and resuspended in buffer containing Fe(II), and Fe(II) oxidation was monitored by the ferrozine assay. When 1 mM initial Fe(II) was provided, approximately 0.8 mM Fe(II) was oxidized within the first half hour with Fe(II)-grown cells, whereas only 0.2 mM Fe(II) was oxidized with H_2- or thiosulfate-grown cells (Fig. 1). Compared to the H_2- or thiosulfate-grown cells,

TABLE 2. Sequences of the oligonucleotides used in this study

Oligonucleotide	Length (bp)	Sequence (5′-3′)[a]
pioA1	28	GGACTAGTCCGACATCGTACTCAACGAC
pioA1p	41	**TATTTAAATTTAGTGGATGGG**TACGAACAG CGACGAGATCC
pioA2	28	GGACTAGTAGTATTGGCCGCTGAGTTTG
pioA2p	42	**CCCATCCACTAAATTTAAATA**TGCCAGAATT GTCACAACAAC
pioB1	28	GGACTAGTGTTACTTCGTCGGCTCCAAG
pioB1p	41	**TATTTAAATTTAGTGGATGGG**TACGGTCAC CACGGAGATTG
pioB2	28	GGACTAGTTCGACGACGAAGGCTTCTAT
pioB2P	41	**CCCATCCACTAAATTTAAATA**GCGCAGTAC TTCCAGGTCTC
pioC1	28	GGACTAGTAACGCCGCTACGACAATTAC
pioC1p	40	**TATTTAAATTTAGTGGATGGG**GTCGTTGCG TTTGTCGTTC
pioC2	28	GGACTAGTTCAGTTCATGTGCCAGCATC
pioC2p	39	**CCCATCCACTAAATTTAAATA**AGCCCGATC AGCGAGAAC
pioA-start	28	GGAAGCTTCCGACATCGTACTCAACGAC
pioA-end	28	GGACTAGTGAGTCGTTCCATCACCCTTC
pioB-start	26	AAGCTTGAACGCTTGCCAGAATTGTC
pioB-end	26	ACTAGTGTCTGTCGTCCTCCCATTGT
pioC-start	28	GGAAGCTTCAGCCAACGTCAACAACAAT
pioC-end	28	GGACTAGTGCAGATGACGTGATCAAAGC
RT-pioA-L1	20	TCAACGACACCTGCTACACC
RT-pioB-R1	20	TTACGGTCACCACGGAGATT
RT-pioB-L1	20	GCGCAGTACTTCCAGGTCTC
RT-pioC-R1	19	GTCGTTGCGTTTGTCGTTC
RT-pioAL	20	AGG TGA TGG ACA CCT GCT TC
RT-pioAR	20	ACG CAG GTG ATT TTC GTT TC
RT-pioBL	20	GCCTGAAGAAGAGCAACACC
RT-pioBR	20	GCATAGCCGAGCTTGAAATC
RT-pioCL	19	GAACGACAAACGCAACGAC
RT-pioCR	19	AGGCCTTCTTGGTGACCTG

[a] The linker regions in the primers for crossover PCR are in bold, and the restriction sites are underlined.

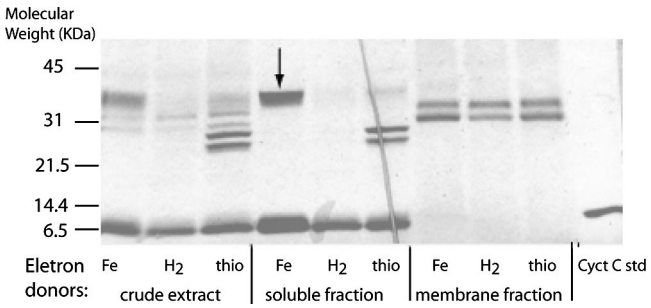

FIG. 2. Heme staining of crude cell extract and soluble and membrane proteins of TIE-1 grown on Fe(II), H_2, and thiosulfate, separated by SDS-PAGE. A *c*-type cytochrome (~40 kDa), indicated by the black arrow, is highly expressed in the soluble fraction of Fe(II)-grown cells. Approximately 100 mg of protein was loaded per lane. The dark diagonal line in the "soluble-fraction thio" lane is a tear in the gel. std, standard.

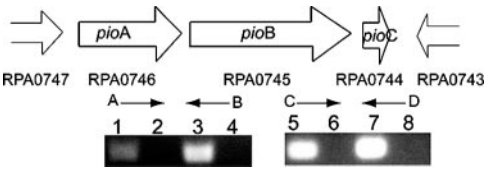

FIG. 3. Organization of the *pio* genes on the *R. palustris* TIE-1 chromosome. Arrows indicate the direction of transcription. The gene numbers corresponding to these genes in *R. palustris* CGA009 are given. The small black arrows A, B, C, and D indicate the locations of primers used for RT-PCR experiments. PCR products were obtained for both of the regions between the *pio* genes, indicating that they constitute an operon. RT reactions, lanes 1 and 5; control with no reverse transcriptase added to cDNA, lanes 2 and 6; TIE-1 genomic DNA control, lanes 3 and 7; no-template control, lanes 4 and 8.

Fe(II)-grown cells showed a four- to fivefold higher rate of Fe(II) oxidation activity, suggesting that specific proteins were induced under Fe(II)-grown conditions. Given these results, we assayed for differential protein expression with cells grown on Fe(II) compared to other electron donors. Crude cell extracts from cells grown on H_2, thiosulfate, or Fe(II) were separated by SDS-PAGE. Although no significant differences were detected visually by Coomassie staining (data not shown), a difference in expression of *c*-type cytochromes was observed by heme staining. Accordingly, we characterized the expression profile of *c*-type cytochromes from soluble and membrane fractions of cells grown on Fe(II), H_2, and thiosulfate (Fig. 2). A unique *c*-type cytochrome (~40 kDa) appeared in significant quantity in the soluble fraction only when cells were grown on Fe(II). Protein identification by mass spectrometry indicated that peptide fragments of this protein match those of a putative decaheme *c*-type cytochrome from *R. palustris* CGA009 (encoded by gene RPA0746) (39).

Identification and sequence analysis of the *pio* genes. By designing primers based on the CGA009 genome, we were able to sequence a 5.7-kb region from TIE-1 that includes the decaheme *c*-type cytochrome open reading frame (ORF), as well as two downstream ORFs (Fig. 3). We designate these genes *pioA*, *pioB*, and *pioC*, where *pio* stands for *p*hototrophic *i*ron *o*xidation. The deduced protein sequences of *pioA*, *pioB*, and *pioC* are about 98%, 97%, and 100% identical to those of RPA0746, RPA0745, and RPA0744, respectively, indicating high sequence similarity between TIE-1 and CGA009 over this region, consistent with the highly conserved sequences previously identified between these two strains (28). To test the hypothesis that genes *pioABC* form an operon, we carried out RT-PCR experiments with primers designed to amplify the intergenic regions. RT-PCR products were obtained for both intergenic regions in the cluster (Fig. 3). No product was obtained in controls from which reverse transcriptase or template DNA was omitted. These results show that *pioABC* are cotranscribed. An intergenic region of about 700 bp is present upstream of *pioA*, preceded by an ORF encoding a protein homologous to a subunit of the putative sulfate ABC transporter CysA from *E. coli* K-12 (27). The ORF downstream of *pioC* transcribes in the opposite direction relative to the *pio* operon. Because of the presence of the large intergenic region upstream of the *pio* operon, as well as the opposite direction of transcription for the downstream ORF, it seems likely that the *pio* operon functions independently of the adjacent genes.

The deduced amino acid sequence of *pioA* consists of 540 amino acids with a putative signal sequence characteristic of secreted proteins through the Sec pathway; a cleavage site is predicted between residues 40 and 41, according to SignalP (http://www.cbs.dtu.dk/services/SignalP/). The lack of hydrophobic regions within PioA, with the exception of the signal sequence, and the observation that PioA is present in the soluble fraction (Fig. 2) suggest that PioA is likely to be a periplasmic protein. PioA contains 10 putative heme-binding sites (CXXCH) characteristic of *c*-type cytochromes. Comparison of PioA to sequences in the NCBI database (http://www.ncbi.nlm.nih.gov/BLAST/) revealed that it is similar to several decaheme *c*-type cytochromes in *Shewanella*, *Vibrio*, and *Geobacter* species (4, 40–43, 48, 51–54). In particular, it has 40% identity and 55% similarity over 285 amino acids to MtrA from *Shewanella oneidensis* MR-1, which is involved in metal [e.g., Fe(III) and Mn(IV)] reduction (5, 49, 50, 58), and this similarity is mostly due to the highly conserved nature of the heme-binding sites that are present close to the C-terminal end of PioA. However, approximately 270 amino acids close to the N terminus of PioA have no homolog in the database. No significant similarity was found when comparing PioA to other proteins in the database.

The second ORF, *pioB*, is 99 nucleotides downstream of *pioA*. *pioB* encodes a protein of 810 amino acids and contains a putative signal peptide with a predicted cleavage site between residues 25 and 26 on the basis of the SignalP program, suggesting that it is also secreted through the Sec pathway. It has a putative porin motif close to the C terminus according to InterProScan (http://www.ebi.ac.uk/InterProScan/) and is predicted to be an outer membrane β-barrel protein according to the Transmembrane Barrel Hunt (20) and PRED-TMBB programs (3). Comparison of PioB to sequences in the databases revealed similarities to several outer membrane proteins from *Shewanella* and *Geobacter* species. In particular, it has 21% identity and 38% similarity over 536 amino acids close to the C terminus of outer membrane protein MtrB from *S. oneidensis* MR-1, which is involved in metal [e.g., Fe(III) and Mn(IV)] reduction (4, 51). However, approximately 120 amino acids at the N terminus show no homology to anything in the database.

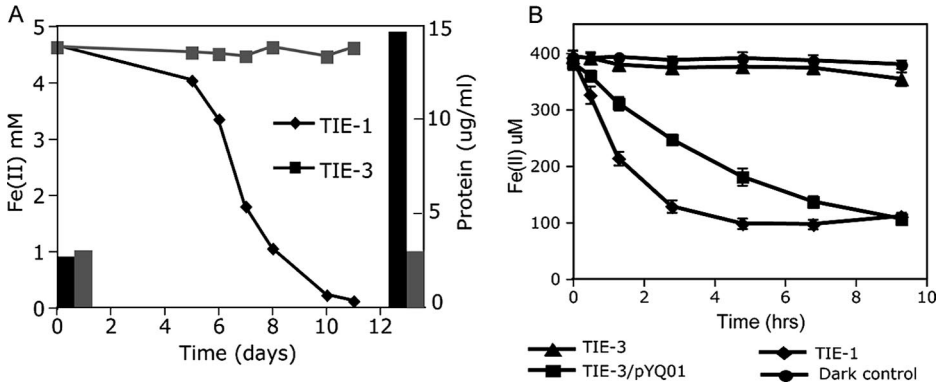

FIG. 4. (A) Defect in growth and phototrophic Fe(II) oxidation in the *pio* operon deletion mutant TIE-3. Data are representative of triplicate cultures. Whereas TIE-1 oxidized Fe(II) to completion in 2 weeks, very little Fe(II) was oxidized by TIE-3. Endpoint measurements of total protein content in these cultures revealed that TIE-3 did not grow during the course of incubation, in contrast to TIE-1. (B) TIE-3 is defective in Fe(II) oxidation activity measured by the cell suspension assay compared to TIE-1. Complementation with the *pio* operon on a plasmid (pYQ01) restored TIE-3's Fe(II) oxidation activity to about 50% of that of TIE-1, whereas a vector (pBBRMCS-2) control had no effect (data not shown).

According to the secondary structure predicted by PRED-TMBB (3), both PioB and MtrB are outer membrane porins with 28 transmembrane beta strands, the largest number of beta strands among all known outer membrane porins (9, 33, 62). Similar to other outer membrane porins, PioB and MtrB are predicted to have long loops protruding into the extracellular space and short turns on the periplasmic side, except that PioB has longer extracellular loops than MtrB, consistent with the sequence length difference between the two proteins. The conserved regions between PioB and MtrB mainly occur in the transmembrane regions, consistent with the idea that these regions are generally more conserved than the loop regions among outer membrane porins (62).

The third ORF, *pioC*, is 140 nucleotides downstream of *pioB*. *pioC* encodes a putative *hi*gh *p*otential *i*ron-sulfur *p*rotein (HiPIP) that contains an iron-sulfur binding site. The deduced amino acid sequence of *pioC* consists of 94 amino acids with a predicted Tat signal sequence at the N terminus, suggesting export into the periplasm through the Tat protein translocation pathway. A signal sequence cleavage site was predicted between residues 37 and 38 on the basis of the SignalP program. Because there is no transmembrane region other than the signal peptide predicted by HMMTOP (http://www.enzim.hu/hmmtop/html/submit.html), we predict that PioC resides in the periplasm. Comparison of PioC to sequences in the database reveals similarities to HiPIPs from several bacteria, with most of the similarity occurring over approximately 50 amino acid residues close to the C terminus spanning the iron-sulfur cluster binding site. PioC is 47% identical and 52% similar over 48 amino acids to a HiPIP from *Rhodopila globiformis* (1), is 32% identical to a hypothetical protein encoded by gene RPA3566 from *R. palustris* CGA009, and is 44% identical and 53% similar over 51 amino acids to a HiPIP from *Acidithiobacillus ferrooxidans*, a putative iron oxidoreductase known as the "Iro" protein (19, 37).

***pioABC* are specifically required for phototrophic Fe(II) oxidation.** To determine whether the *pio* operon is necessary for growth on Fe(II), we constructed a mutant (TIE-3) in which all three genes in the *pio* operon were deleted from the chromosome by homologous recombination. We tested the ability of mutant TIE-3 to grow on different substrates. When Fe(II) was provided as the electron donor for photoautotrophic growth, very little Fe(II) was oxidized by strain TIE-3 in a period of 2 weeks (Fig. 4A). In contrast, wild-type strain TIE-1 oxidized Fe(II) to completion within this time period. Endpoint measurements of total protein content in the cultures indicated that TIE-3 did not grow over the course of incubation, in contrast to TIE-1 (Fig. 4A). To determine if TIE-3 was specifically defective for growth on Fe(II), we tested growth on substrates other than Fe(II). Photoautotrophic growth of TIE-3 on H_2 or thiosulfate and photoheterotrophic growth on acetate were tested by measuring cell OD. TIE-3 grew on these substrates as well as TIE-1 (Table 3). These results indicate that the *pioABC* operon is essential and specific for growth on Fe(II).

To further characterize the *pioABC* operon deletion mutant with respect to its Fe(II) oxidation phenotype, we performed a cell suspension assay. In this assay, H_2-grown wide-type and mutant TIE-3 cells were washed and then incubated with Fe(II) under light in an anaerobic chamber. Fe(II) oxidation activity was followed by ferrozine assay. The Fe(II) oxidation activity we observed was light dependent (Fig. 4B). Over a period of several hours for the equivalent density of H_2-grown cells, 400 μM Fe(II) was oxidized to completion by TIE-1 but very little Fe(II) was oxidized by TIE-3. This indicates that the *pio* operon is responsible for almost all of the Fe(II) oxidation activity in H_2-grown TIE-1. Considering the initial rate of Fe(II) oxidation, the activity of TIE-3 could be restored to

TABLE 3. Comparison of the doubling times of *R. palustris* TIE-1 and TIE-3 grown on different substrates

Substrate	Doubling time (h)	
	TIE-1	TIE-3
Fe(II)	80 ± 10	—[a]
H_2	40 ± 5	36 ± 7
Thiosulfate	55 ± 7	57 ± 6
Acetate	8 ± 2	8 ± 3

[a] —, no-growth observed.

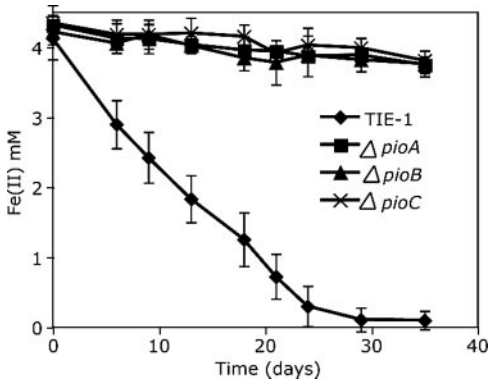

FIG. 5. Fe(II) oxidation by individual *pio* deletion mutants (Δ*pioA*, Δ*pioB*, and Δ*pioC*) when Fe(II) is provided as the sole electron donor. Data are representative of triplicate cultures. Whereas the wild type (TIE-1) oxidized Fe(II) to completion within 3 weeks, very little Fe(II) was oxidized by each mutant. No growth occurred for any of these mutants on the basis of measurement of protein content (data not shown).

about 50% of the wide-type level by complementation with the entire *pio* operon (Fig. 4B); the total amount of Fe(II) that was oxidized over a period of 9 h was the same between wide-type TIE-1 and the complemented strain. The vector alone did not affect Fe(II) oxidation by TIE-3 or TIE-1 (data not shown). However, complementation with each individual gene (*pioA*, *pioB*, or *pioC*) did not restore any Fe(II) oxidation activity (data not shown). This suggests that more than one gene in the *pio* operon is necessary for this activity.

Because the *pio* operon is so highly conserved between strains CGA009 and TIE-1, we checked whether the *pio* operon also confers Fe(II) oxidation on CGA010. Deletion of the genes corresponding to *pioABC* (i.e., RPA0746, RPA0745, and RPA0744) in CGA010 resulted in a large defect in Fe(II) oxidation activity (data not shown), similar to that observed in TIE-1. Strain CGA010 shows a similar amount of Fe(II) oxidation activity in the cell suspension assay as H_2-grown TIE-1. However, it does not show measurable growth over the same time period as TIE-1; therefore, we chose to work with strain TIE-1 for further analysis.

To access the relative importance of the individual *pio* genes for Fe(II) oxidation, we constructed three individual deletion mutants, Δ*pioA*, Δ*pioB*, and Δ*pioC*. We confirmed that the mutations were nonpolar by RT-PCR (data not shown) with the primers listed in Table 2. Neither growth nor Fe(II) oxidation occurred for any of these mutants during a growth assay on Fe(II) (Fig. 5); growth of these mutants on other substrates such as H_2, thiosulfate, or acetate was unaffected (data not shown). In contrast, Δ*pioA* lost almost all Fe(II) oxidation activity in the cell suspension assay with H_2-grown cells, similar to TIE-3, whereas Δ*pioB* and Δ*pioC* only partially lost Fe(II) oxidation activity, exhibiting approximately 10% and 40% of the initial wild-type rate of Fe(II) oxidation (Fig. 6A). The partial defect in Fe(II) oxidation by Δ*pioC* may be explained by functional substitution of other small soluble electron carriers in the cell (e.g., the other HiPIP encoded by the homolog of RPA3566). Complementation by the respective wild-type copies of the genes restored Fe(II) oxidation activity to different extents in the mutants. In comparing the total amounts of Fe(II) oxidized after 12 h, complementation of Δ*pioA*, Δ*pioB*, and Δ*pioC* resulted in 85, 60, and 99% of that achieved by TIE-1 in the same amount of time (Fig. 6B). The reason for the relatively low extent of complementation for Δ*pioB* compared to TIE-1 is not clear. Perhaps it is caused by different levels of expression of *pioB* when expressed on a vector driven by a nonnative promoter versus when expressed from the endogenous promoter. Together, these results indicate that all three Pio proteins are required for full Fe(II) oxidation activity in *R. palustris* TIE-1.

DISCUSSION

Iron is thought to have been an important substrate for microbial metabolism on the early Earth, including ancient types of photosynthesis. Although the molecular basis of Fe(II) oxidation by acidophilic bacteria has been studied for decades (67, 68, 74, 75, 77), it is only very recently that Fe(II) oxidation

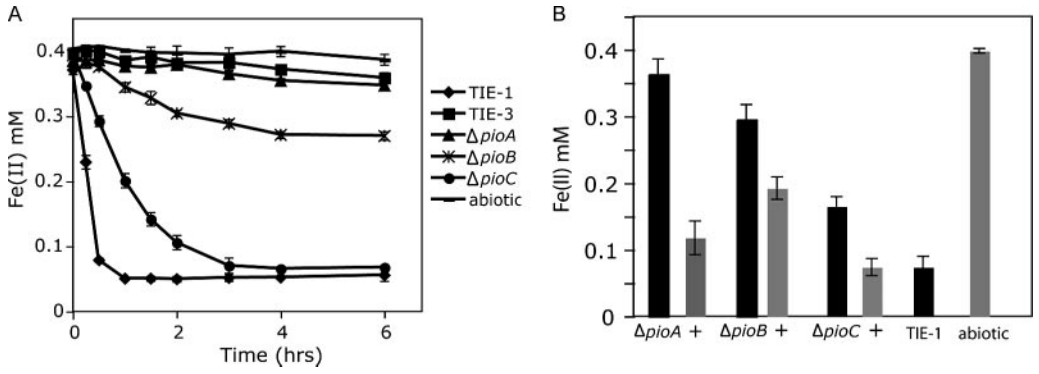

FIG. 6. (A) Fe(II) oxidation activity by individual *pio* deletion mutants (Δ*pioA*, Δ*pioB*, and Δ*pioC*) in the cell suspension assay. Δ*pioA* lost nearly all of its Fe(II) oxidation activity, similar to the *pio* operon deletion mutant TIE-3. The Δ*pioB* and Δ*pioC* mutants showed approximately 10% and 40% of the activity of TIE-1 [as measured by calculating the rate of Fe(II) oxidation in the linear portion of the curve]. Data represent the mean ± standard deviation of three independent cultures. (B) Complementation by the respective wild-type copies of the *pio* genes restored Fe(II) oxidation activity to different extents in the mutants. In comparing the total amounts of Fe(II) oxidized after 12 h, complementation of Δ*pioA*, Δ*pioB*, and Δ*pioC* resulted in 85, 60, and 99% of that achieved by TIE-1 in the same amount of time.

has been examined in anoxygenic phototrophs (11, 28). Because photoautotrophic Fe(II) oxidation is likely to have been one of the most ancient forms of microbial Fe(II) oxidation (12), understanding the molecular basis of this metabolism is relevant not only for understanding the evolution of photosynthesis but also for understanding the evolution of other Fe(II)-oxidation systems.

c-type cytochromes with a wide range of redox potentials are involved in Fe(II) oxidation by *A. ferrooxidans* (2, 68, 76, 77) and *Rhodobacter* sp. strain SW2 (11), as well as dissimilatory Fe(III) reduction by *Shewanella* and *Geobacter* species (4, 40, 42, 43, 73). Consistent with this, we found a *c*-type cytochrome to be upregulated when *R. palustris* TIE-1 was grown photoautotrophically on Fe(II). By reverse genetic analysis, we identified a three-gene operon (the *pio* operon) that seems likely to encode the phototrophic Fe(II) oxidoreductase complex. Detailed biochemical studies are needed to confirm this and understand the mechanism of electron transfer from Fe(II); however, on the basis of the results of this study, we can suggest potential functions for the Pio proteins.

The first gene in the *pio* operon encodes PioA, a putative decaheme *c*-type cytochrome. Because the Δ*pioA* mutant lost almost all of its Fe(II) oxidation activity, similar to the *pio* operon deletion mutant TIE-3, this suggests that PioA plays an essential role during Fe(II) oxidation. We postulate that it receives electrons directly from Fe(II), serving as the Fe(II) oxidoreductase. This function would be analogous to that of *c*-type cytochromes in *S. oneidensis* and in *A. ferrooxidans* (2, 54) that serve as the electron donor to Fe(III) and direct electron acceptors from Fe(II), respectively. Although confirmation of protein localization is necessary, sequence analyses suggest that PioA is a soluble protein that resides in the periplasm.

The second gene in the operon encodes PioB, a putative outer membrane beta barrel protein with no obvious redox active prosthetic groups. While not as severe as the phenotype produced by Δ*pioA*, deletion of *pioB* caused a large defect in Fe(II) oxidation, suggesting that PioB also plays an important role in this process. We suggest that it functions as an iron transporter, given its similarity to other known outer membrane porins (55, 62) and its lack of redox-cofactor binding motifs. However, neither the transport direction nor the substrate [e.g., an Fe(II) or Fe(III) complex] of PioB is known. The closest relative of PioB is MtrB from *S. oneidensis* MR-1, which is involved in dissimilatory Fe(III) reduction (4, 48, 51, 52, 54). It has been suggested that MtrB helps localize the Fe(III) reductase complex in *S. oneidensis* MR-1 to the outside of the cell (51). By analogy, it is also possible that PioB may assist in the localization of other proteins involved in Fe(II) oxidation that remain to be identified.

The third gene in the operon encodes PioC, a putative HiPIP. Given that PioC is required for growth on Fe(II), we suggest that it functions as an electron carrier from PioA to the photosynthetic reaction center (RC). On the basis of the measured redox potential of a HiPIP (0.345 V) from *Rhodopseudomonas marina* (23, 47), the calculated iron couple $Fe(OH)_3$-Fe^{2+} (−1.1 V) (28) and the measured RC (0.4 to 0.5 V) in purple bacteria (57), a HiPIP is a reasonable candidate for this function because its redox potential falls between those of the iron couple and the RC. Spectroscopic and kinetic experiments have shown that HiPIPs can mediate electron transfer to the RC directly or via an RC-bound cytochrome in various purple bacteria (24, 25, 45, 46, 61). In this way, HiPIPs can functionally substitute for cytochrome c_2, a common electron carrier in the periplasm of purple bacteria that shuttles electrons between the cytochrome *bc1* complex and the RC during cyclic electron flow (47). In the case of *R. palustris* CGA009, genome annotation predicts the presence of cytochrome c_2 (encoded by gene RPA1535), along with another HiPIP (encoded by gene RPA3566). The fact that Δ*pioC* does not have a phototrophic growth defect on H_2 suggests that PioC has a function specific for Fe(II) phototrophy. Interestingly, a HiPIP has been demonstrated to serve as the electron acceptor for a thiosulfate-tetrathionate oxidoreductase during phototrophic growth of *Chromatium vinosum* on thiosulfate (18). PioC is also homologous to a HiPIP (Iro) found in *A. ferrooxidans*, an acidophilic Fe(II)-oxidizing bacterium that couples Fe(II) oxidation to the reduction of oxygen at low pH. Because of its high redox potential, its in vitro ability to oxidize Fe(II) and donate electrons to cytochrome c_{552}, and its stability under acidic conditions, Iro was proposed to catalyze Fe(II) oxidation in *A. ferrooxidans* (19, 37); whether this applies in vivo has been disputed, however (76, 77). Nevertheless, the finding that a HiPIP is involved in Fe(II) oxidation in both *R. palustris* and *A. ferrooxidans* suggests some evolutionary relationship between the two Fe(II) oxidation systems.

In summary, the *pio* operon appears to encode proteins that are responsible for Fe(II) oxidation in *R. palustris* TIE-1. Determining their cellular localization will be important for gaining insight into how this organism traffics in iron. Although much is understood about iron acquisition for assimilatory purposes when iron is limiting (70), *R. palustris* presents an opportunity to understand the opposite problem: how does a cell dispose of Fe(III) when it is growing on Fe(II)? Interestingly, in phototrophic Fe(II)-oxidizing bacteria, the Fe(III) mineral product appears to be deposited exclusively outside the cell (28, 29); this makes sense because precipitation of ferric minerals inside the cell could be fatal given the highly insoluble nature of Fe(III) at neutral pH. If our predictions are correct and the Fe(II) oxidoreductase complex resides in the periplasm, how then does the cell avoid this problem? Are there specific ligands that keep Fe(III) soluble? Or are there protein complexes that bind and transport Fe(III) out of the cell so efficiently that internal ferric mineral precipitation is precluded? We hope that future biochemical studies of the Pio proteins and their associated partners will address these questions.

ACKNOWLEDGMENTS

We give special thanks to C. Romano and S. Potter for help in sequencing *pioA* and *pioB*. We thank D. Lies and L. Dietrich for guidance throughout this study; D. Lies, N. Caizza, and C. Romano for comments on the manuscript; and all the Newman lab members for helpful discussions.

This work was supported by grants from the Packard Foundation and the Howard Hughes Medical Institute to D.K.N.

REFERENCES

1. **Ambler, R. P., T. E. Meyer, and M. D. Kamen.** 1993. Amino-acid-sequence of a high redox potential ferredoxin (HiPIP) from the purple phototrophic bacterium Rhodopila globiformis, which has the highest known redox potential of its class. Arch. Biochem. Biophys. **306:**215–222.
2. **Appia-Ayme, C., A. Bengrine, C. Cavazza, M. T. Giudici-Orticoni, M. Bruschi,**

M. Chippaux, and V. Bonnefoy. 1998. Characterization and expression of the cotranscribed *cyc1* and *cyc2* genes encoding the cytochrome c_4 (c_{552}) and a high-molecular-mass cytochrome *c* from *Thiobacillus ferrooxidans* ATCC 33020. FEMS Microbiol. Lett. **167:**171–177.

3. **Bagos, P. G., T. D. Liakopoulos, I. C. Spyropoulos, and S. J. Hamodrakas.** 2004. A hidden Markov model method, capable of predicting and discriminating beta-barrel outer membrane proteins. BMC Bioinformatics **5:**29.
4. **Beliaev, A. S., and D. A. Saffarini.** 1998. *Shewanella putrefaciens mtrB* encodes an outer membrane protein required for Fe(III) and Mn(IV) reduction. J. Bacteriol. **180:**6292–6297.
5. **Beliaev, A. S., D. A. Saffarini, J. L. McLaughlin, and D. Hunnicutt.** 2001. MtrC, an outer membrane decahaem *c*-type cytochrome required for metal reduction in Shewanella putrefaciens MR-1. Mol. Microbiol. **39:**722–730.
6. **Blankenship, R. E.** 1992. Origin and early evolution of photosynthesis. Photosynth. Res. **33:**91–111.
7. **Bradford, M. M.** 1976. Rapid and sensitive method for quantitation of microgram quantities of protein utilizing principle of protein-dye binding. Anal. Biochem. **72:**248–254.
8. **Buchanan, B. B.** 1992. Carbon-dioxide assimilation in oxygenic and anoxygenic photosynthesis. Photosynth. Res. **33:**147–162.
9. **Buchanan, S. K., B. S. Smith, L. Venkatramani, D. Xia, L. Esser, M. Palnitkar, R. Chakraborty, D. van der Helm, and J. Deisenhofer.** 1999. Crystal structure of the outer membrane active transporter FepA from Escherichia coli. Nat. Struct. Biol. **6:**56–63.
10. **Croal, L. R., J. A. Gralnick, D. Malasarn, and D. K. Newman.** 2004. The genetics of geochemistry. Annu. Rev. Genet. **38:**175–202.
11. **Croal, L. R., Y. Jiao, and D. K. Newman.** 2007. The *fox* operon from *Rhodobacter* strain SW2 promotes phototrophic Fe(II) oxidation in *Rhodobacter capsulatus* SB1003. J. Bacteriol. **189:**1774–1782.
12. **Croal, L. R., C. M. Johnson, B. L. Beard, and D. K. Newman.** 2004. Iron isotope fractionation by Fe(II)-oxidizing photoautotrophic bacteria. Geochim. Cosmochim. Acta **68:**1227–1242.
13. **Egland, P. G., J. Gibson, and C. S. Harwood.** 1995. Benzoate-coenzyme A ligase, encoded by *badA*, is one of three ligases able to catalyze benzoyl-coenzyme a formation during anaerobic growth of *Rhodopseudomonas palustris* on benzoate. J. Bacteriol. **177:**6545–6551.
14. **Ehrenreich, A., and F. Widdel.** 1994. Anaerobic oxidation of ferrous iron by purple bacteria, a new-type of phototrophic metabolism. Appl. Environ. Microbiol. **60:**4517–4526.
15. **Farquhar, J., H. M. Bao, and M. Thiemens.** 2000. Atmospheric influence of Earth's earliest sulfur cycle. Science **289:**756–758.
16. **Francis, R. T., and R. R. Becker.** 1984. Specific indication of hemoproteins in polyacrylamide gels using a double-staining process. Anal. Biochem. **136:** 509–514.
17. **Friedrich, C. G.** 1998. Physiology and genetics of sulfur-oxidizing bacteria. Adv. Microb. Physiol. **39:**235–289.
18. **Fukumori, Y., and T. Yamanaka.** 1979. High-potential non-heme iron protein (HiPIP)-linked, thiosulfate-oxidizing enzyme derived from Chromatium vinosum. Curr. Microbiol. **3:**117–120.
19. **Fukumori, Y., T. Yano, A. Sato, and T. Yamanaka.** 1988. Fe(II)-oxidizing enzyme purified from *Thiobacillus ferrooxidans*. FEMS Microbiol. Lett. **50:** 169–172.
20. **Garrow, A. G., A. Agnew, and D. R. Westhead.** 2005. TMB-Hunt: an amino acid composition based method to screen proteomes for beta-barrel transmembrane proteins. BMC Bioinformatics **6:**56.
21. **Heising, S., L. Richter, W. Ludwig, and B. Schink.** 1999. *Chlorobium ferrooxidans* sp. nov., a phototrophic green sulfur bacterium that oxidizes ferrous iron in coculture with a "*Geospirillum*" sp. strain. Arch. Microbiol. **172:**116–124.
22. **Heising, S., and B. Schink.** 1998. Phototrophic oxidation of ferrous iron by a *Rhodomicrobium vannielii* strain. Microbiology **144:**2263–2269.
23. **Henseler, A., H. G. Truper, and U. Fischer.** 1986. Soluble cytochromes of Rhodopseudomonas marina. FEMS Microbiol. Lett. **33:**1–8.
24. **Hochkoeppler, A., S. Ciurli, G. Venturoli, and D. Zannoni.** 1995. The high-potential iron-sulfur protein (HiPIP) from Rhodoferax fermentans is competent in photosynthetic electron transfer. FEBS Lett. **357:**70–74.
25. **Hochkoeppler, A., D. Zannoni, S. Ciurli, T. E. Meyer, M. A. Cusanovich, and G. Tollin.** 1996. Kinetics of photo-induced electron transfer from high-potential iron-sulfur protein to the photosynthetic reaction center of the purple phototroph Rhodoferax fermentans. Proc. Natl. Acad. Sci. USA **93:**6998–7002.
26. **Holland, H. D.** 1973. Oceans: possible source of iron in iron formations. Economic Geology **68:**1169–1172.
27. **Hryniewicz, M., A. Sirko, A. Palucha, A. Bock, and D. Hulanicka.** 1990. Sulfate and thiosulfate transport in *Escherichia coli* K-12: identification of a gene encoding a novel protein involved in thiosulfate binding. J. Bacteriol. **172:**3358–3366.
28. **Jiao, Y., A. Kappler, L. R. Croal, and D. K. Newman.** 2005. Isolation and characterization of a genetically tractable photoautotrophic Fe(II)-oxidizing bacterium, *Rhodopseudomonas palustris* strain TIE-1. Appl. Environ. Microbiol. **71:**4487–4496.
29. **Kappler, A., and D. K. Newman.** 2004. Formation of Fe(III)-minerals by Fe(II)-oxidizing photoautotrophic bacteria. Geochim. Cosmochim. Acta **68:** 1217–1226.
30. **Karhu, J. A., and H. D. Holland.** 1996. Carbon isotopes and the rise of atmospheric oxygen. Geology **24:**867–870.
31. **Keen, N. T., S. Tamaki, D. Kobayashi, and D. Trollinger.** 1988. Improved broad-host-range plasmids for DNA cloning in gram-negative bacteria. Gene **70:**191–197.
32. **Kim, M. K., and C. S. Harwood.** 1991. Regulation of benzoate-CoA ligase in *Rhodopseudomonas palustris*. FEMS Microbiol. Lett. **83:**199–203.
33. **Koebnik, R., K. P. Locher, and P. Van Gelder.** 2000. Structure and function of bacterial outer membrane proteins: barrels in a nutshell. Mol. Microbiol. **37:**239–253.
34. **Konhauser, K. O., T. Hamade, R. Raiswell, R. C. Morris, F. G. Ferris, G. Southam, and D. E. Canfield.** 2002. Could bacteria have formed the Precambrian banded iron formations? Geology **30:**1079–1082.
35. **Kovach, M. E., P. H. Elzer, D. S. Hill, G. T. Robertson, M. A. Farris, R. M. Roop, and K. M. Peterson.** 1995. Four new derivatives of the broad-host-range cloning vector pBBR1MCS, carrying different antibiotic resistance cassettes. Gene **166:**175–176.
36. **Kovach, M. E., R. W. Phillips, P. H. Elzer, R. M. Roop, and K. M. Peterson.** 1994. pBBR1MCS: a broad-host-range cloning vector. BioTechniques **16:** 800–802.
37. **Kusano, T., T. Takeshima, K. Sugawara, C. Inoue, T. Shiratori, T. Yano, Y. Fukumori, and T. Yamanaka.** 1992. Molecular cloning of the gene encoding Thiobacillus ferrooxidans Fe(II) oxidase: high homology of the gene-product with HiPIP. J. Biol. Chem. **267:**11242–11247.
38. **Laemmli, U. K.** 1970. Cleavage of structural proteins during the assembly of the head of bacteriophage T4. Nature **227:**680–685.
39. **Larimer, F. W., P. Chain, L. Hauser, J. Lamerdin, S. Malfatti, L. Do, M. L. Land, D. A. Pelletier, J. T. Beatty, A. S. Lang, F. R. Tabita, J. L. Gibson, T. E. Hanson, C. Bobst, J. Torres, C. Peres, F. H. Harrison, J. Gibson, and C. S. Harwood.** 2004. Complete genome sequence of the metabolically versatile photosynthetic bacterium *Rhodopseudomonas palustris*. Nat. Biotechnol. **22:** 55–61.
40. **Leang, C., L. A. Adams, K. J. Chin, K. P. Nevin, B. A. Methe, J. Webster, M. L. Sharma, and D. R. Lovley.** 2005. Adaptation to disruption of the electron transfer pathway for Fe(III) reduction in *Geobacter sulfurreducens*. J. Bacteriol. **187:**5918–5926.
41. **Leang, C., M. V. Coppi, and D. R. Lovley.** 2003. OmcB, a *c*-type polyheme cytochrome, involved in Fe(III) reduction in *Geobacter sulfurreducens*. J. Bacteriol. **185:**2096–2103.
42. **Leang, C., and D. R. Lovley.** 2005. Regulation of two highly similar genes, omcB and omcC, in a 10 kb chromosomal duplication in Geobacter sulfurreducens. Microbiology **151:**1761–1767.
43. **Lies, D. P., M. E. Hernandez, A. Kappler, R. E. Mielke, J. A. Gralnick, and D. K. Newman.** 2005. *Shewanella oneidensis* MR-1 uses overlapping pathways for iron reduction at a distance and by direct contact under conditions relevant for biofilms. Appl. Environ. Microbiol. **71:**4414–4426.
44. **Madigan, M. T., J. M. Martinko, and J. Parker.** 2002. Brock biology of microorganisms, 10th ed. p. A-4. Prentice Hall, Englewood Cliffs, NJ.
45. **Menin, L., J. Gaillard, P. Parot, B. Schoepp, W. Nitschke, and A. Vermeglio.** 1998. Role of HiPIP as electron donor to the RC-bound cytochrome in photosynthetic purple bacteria. Photosynth. Res. **55:**343–348.
46. **Menin, L., B. Schoepp, P. Parot, and A. Vermeglio.** 1997. Photoinduced cyclic electron transfer in Rhodocyclus tenuis cells: participation of HiPIP or cyt c_8 depending on the ambient redox potential. Biochemistry **36:**12183–12188.
47. **Meyer, T. E., and M. A. Cusanovich.** 2003. Discovery and characterization of electron transfer proteins in the photosynthetic bacteria. Photosynth. Res. **76:**111–126.
48. **Myers, C. R., and J. M. Myers.** 2003. Cell surface exposure of the outer membrane cytochromes of Shewanella oneidensis MR-1. Lett. Appl. Microbiol. **37:**254–258.
49. **Myers, C. R., and J. M. Myers.** 1993. Ferric reductase is associated with the membranes of anaerobically grown Shewanella putrefaciens MR-1. FEMS Microbiol. Lett. **108:**15–22.
50. **Myers, C. R., and J. M. Myers.** 1992. Localization of cytochromes to the outer membrane of anaerobically grown *Shewanella putrefaciens* MR-1. J. Bacteriol. **174:**3429–3438.
51. **Myers, C. R., and J. M. Myers.** 2002. MtrB is required for proper incorporation of the cytochromes OmcA and OmcB into the outer membrane of *Shewanella putrefaciens* MR-1. Appl. Environ. Microbiol. **68:**5585–5594.
52. **Myers, C. R., and J. M. Myers.** 2004. The outer membrane cytochromes of Shewanella oneidensis MR-1 are lipoproteins. Lett. Appl. Microbiol. **39:**466–470.
53. **Myers, J. M., and C. R. Myers.** 2003. Overlapping role of the outer membrane cytochromes of Shewanella oneidensis MR-1 in the reduction of manganese(IV) oxide. Lett. Appl. Microbiol. **37:**21–25.
54. **Myers, J. M., and C. R. Myers.** 2001. Role for outer membrane cytochromes OmcA and OmcB of *Shewanella putrefaciens* MR-1 in reduction of manganese dioxide. Appl. Environ. Microbiol. **67:**260–269.

55. **Nikaido, H.** 2003. Molecular basis of bacterial outer membrane permeability revisited. Microbiol. Mol. Biol. Rev. **67:**593–656.
56. **Oda, Y., S. K. Samanta, F. E. Rey, L. Y. Wu, X. D. Liu, T. F. Yan, J. Z. Zhou, and C. S. Harwood.** 2005. Functional genomic analysis of three nitrogenase isozymes in the photosynthetic bacterium *Rhodopseudomonas palustris*. J. Bacteriol. **187:**7784–7794.
57. **Olson, J. M., and R. E. Blankenship.** 2004. Thinking about the evolution of photosynthesis. Photosynth. Res. **80:**373–386.
58. **Pitts, K. E., P. S. Dobbin, F. Reyes-Ramirez, A. J. Thomson, D. J. Richardson, and H. E. Seward.** 2003. Characterization of the Shewanella oneidensis MR-1 decaheme cytochrome MtrA. J. Biol. Chem. **278:**27758–27765.
59. **Quandt, J., and M. F. Hynes.** 1993. Versatile suicide vectors which allow direct selection for gene replacement in gram-negative bacteria. Gene **127:** 15–21.
60. **Rasmussen, B., and R. Buick.** 1999. Redox state of the archean atmosphere: evidence from detrital heavy minerals in ca. 3250-2750 Ma sandstones from the Pilbara Craton, Australia. Geology **27:**115–118.
61. **Schoepp, B., P. Parot, L. Menin, J. Gaillard, P. Richaud, and A. Vermeglio.** 1995. *In-vivo* participation of a high-potential iron-sulfur protein as electron-donor to the photochemical-reaction center of Rubrivivax gelatinosus. Biochemistry **34:**11736–11742.
62. **Schulz, G. E.** 2002. The structure of bacterial outer membrane proteins. Biochim. Biophys. Acta **1565:**308–317.
63. **Simon, R., U. Priefer, and A. Puhler.** 1983. A broad host range mobilization system for *in-vivo* genetic engineering: transposon mutagenesis in gram-negative bacteria. Bio-Technology **1:**784–791.
64. **Stookey, L. L.** 1970. Ferrozine—a new spectrophotometric reagent for iron. Anal. Chem. **42:**779–781.
65. **Straub, K. L., M. Benz, and B. Schink.** 2001. Iron metabolism in anoxic environments at near neutral pH. FEMS Microbiol. Ecol. **34:**181–186.
66. **Straub, K. L., F. A. Rainey, and F. Widdel.** 1999. *Rhodovulum iodosum* sp. nov. and *Rhodovulum robiginosum* sp. nov., two new marine phototrophic ferrous-iron-oxidizing purple bacteria. Int. J. Syst. Bacteriol. **49:**729–735.
67. **Temple, K. L., and A. R. Colmer.** 1951. The autotrophic oxidation of iron by a new bacterium, *Thiobacillus ferrooxidans*. J. Bacteriol. **62:**605–611.
68. **Valkova-Valchanova, M. B., and S. H. P. Chan.** 1994. Purification and characterization of two new *c*-type cytochromes involved in Fe^{2+} oxidation from *Thiobacillus ferrooxidans*. FEMS Microbiol. Lett. **121:**61–69.
69. **Walker, J. C. G., C. Klein, M. Schidlowski, J. W. Schopf, D. J. Stevenson, and M. R. Walter.** 1983. Environmental evolution of the archean-early Proterozoic Earth, p. 260–290. *In* J. W. Schopf (ed.), Earth's earliest biosphere. Its origin and evolution. Princeton University Press, Princeton, NJ.
70. **Wandersman, C., and P. Delepelaire.** 2004. Bacterial iron sources: from siderophores to hemophores. Ann. Rev. Microbiol. **58:**611–647.
71. **Widdel, F., S. Schnell, S. Heising, A. Ehrenreich, B. Assmus, and B. Schink.** 1993. Ferrous iron oxidation by anoxygenic phototrophic bacteria. Nature **362:**834–836.
72. **Xiong, J., W. M. Fischer, K. Inoue, M. Nakahara, and C. E. Bauer.** 2000. Molecular evidence for the early evolution of photosynthesis. Science **289:** 1724–1730.
73. **Xiong, Y., L. Shi, B. Chen, M. U. Mayer, B. H. Lower, Y. Londer, S. Bose, M. F. Hochella, J. K. Fredrickson, and T. C. Squier.** 2006. High-affinity binding and direct electron transfer to solid metals by the Shewanella oneidensis MR-1 outer membrane *c*-type cytochrome OmcA. J. Am. Chem. Soc. **128:**13978–13979.
74. **Yamanaka, T., and Y. Fukumori.** 1995. Molecular aspects of the electron transfer system which participates in the oxidation of ferrous ion by *Thiobacillus ferrooxidans*. FEMS Microbiol. Rev. **17:**401–413.
75. **Yamanaka, T., T. Yano, M. Kai, H. Tamegai, A. Sato, and Y. Fukumori.** 1991. The electron transfer system in an acidophilic iron-oxidizing bacterium, p. 223–246. *In* Y. Mukohata (ed.), In new era of bioenergetics. Academic Press, Tokyo, Japan.
76. **Yarzábal, A., C. Appia-Ayme, J. Ratouchniak, and V. Bonnefoy.** 2004. Regulation of the expression of the *Acidithiobacillus ferrooxidans rus* operon encoding two cytochromes *c*, a cytochrome oxidase and rusticyanin. Microbiology **150:**2113–2123.
77. **Yarzábal, A., G. Brasseur, J. Ratouchniak, K. Lund, D. Lemesle-Meunier, J. A. DeMoss, and V. Bonnefoy.** 2002. The high-molecular-weight cytochrome *c* Cyc2 of *Acidithiobacillus ferrooxidans* is an outer membrane protein. J. Bacteriol. **184:**313–317.